Assessment of metal sintering in the copper-zeolite hybrid catalyst for direct dimethyl ether synthesis using synchrotron-based X-ray absorption and diffraction

Andrei Khodakov, Vitaly Ordomsky, Ana Palčić, Mengdie Cai, Vijayanand Subramanian, Yuan Luo, Valentin Valtchev, Simona Moldovan, Ovidiu Ersen

Assessment of metal sintering in the copper-zeolite hybrid catalyst for direct dimethyl ether synthesis using synchrotron-based X-ray absorption and diffraction

Andrei Y. Khodakov[a], Vitaly V. Ordomsky[a], Ana Palčić[b, c], Mengdie Cai[a], Vijayanand Subramanian[a], Yuan Luo[a], Valentin Valtchev[b], Simona Moldovan[d] and Ovidiu Ersen[d]*

[a]*Univ. Lille, CNRS, Centrale Lille, ENSCL, Univ. Artois, UMR 8181 - UCCS - Unité de Catalyse et Chimie du Solide, F-59000 Lille, France.*

[b]*Normandie Univ, ENSICAEN, UNICAEN, CNRS, Laboratoire Catalyse et Spectrochimie, 6 boulevard Maréchal Juin, 14000 Caen, France*

[c]*Laboratory for the Synthesis of New Materials, Division of Materials Chemistry, Ruđer Bošković Institute, Bijenička 54, 10000 Zagreb, Croatia*

[d]*IPCMS, Université de Strasbourg, 23, rue du Loess BP 43, F-67034 Strasbourg, France*

**Corresponding author: andrei.khodakov@univ-lille.fr*

Abstract

Dimethyl ether is one of the most promising environmentally optimized alternatives to the conventional fossil fuels and an important platform molecule for chemical industry. Catalyst deactivation is one of the most important challenges of the single-step dimethyl ether synthesis from syngas. Because of the lack of direct characterization techniques working under harsh reaction conditions, the information about deactivation mechanisms of bifunctional Cu/ZSM-5 catalysts is rather contradictory. In this paper, a combination of synchrotron-based *in-situ* time-resolved X-ray diffraction and X-ray absorption spectroscopy operating under high pressure and temperature alongside with the conventional *ex-situ* characterization uncovered very rapid copper sintering occurring under realistic conditions of direct dimethyl ether synthesis. Copper sintering was strongly affected by the presence of water either produced by the reaction or co-fed to the reactor. No copper oxidation was observed under a wide range of experimental conditions.

Keywords: syngas; dimethyl ether; hybrid catalyst; deactivation; zeolite; hydrogenation

1. Introduction

Dimethyl ether (DME) is one of the most promising environmentally optimized alternatives to the conventional diesel fuels due to its high cetane index (> 55), low emission of CO, NO_x and particulates and reduced noise [1, 2, 3, 4]. DME, which is biodegradable in air, non-carcinogen and non-corrosive, can be also used as a substitute for liquefied petroleum gas (LPG). DME is also an important intermediate for the production of useful chemicals (i.e. methyl acetate and dimethyl sulphate) and petrochemicals (light olefins, BTX aromatics). From the viewpoint of CO_2 emissions, synthesis of DME from renewable feedstocks ("bio-DME") is particularly attractive. In the industry, DME synthesis traditionally proceeds as a two stages process: methanol synthesis from syngas followed by methanol dehydration. The maximum syngas conversion to methanol is limited by thermodynamics especially at high temperatures [5].

At least, three reactions are involved in DME synthesis:

(i) Methanol synthesis: $CO + 2H_2 \rightarrow CH_3OH$. Several reports suggest that methanol synthesis proceeds via intermediate formation of CO_2 [6, 7].

(ii) Dehydration of methanol to DME and water: $2CH_3OH \rightarrow CH_3OCH_3 + H_2O$.

(iii) Water gas shift reaction (WGS), which could modify partial pressures in the reactor: $CO + H_2O \rightarrow CO_2 + H_2$.

Direct DME synthesis overcomes the thermodynamic constraints of the two-stage process and leads to higher DME productivity. In the direct DME synthesis, the reaction occurs in a single reactor under high pressures and temperatures over a bifunctional catalyst, which contains simultaneously active phases for carbon monoxide hydrogenation to methanol and methanol dehydration to DME. Methanol synthesis occurs on copper-based catalysts, while methanol dehydration involves acid catalysts. Copper metal nanoparticles associated with a promoter, i.e. Zn, are usually considered as active phase for methanol synthesis. The advantages of the Cu/Zn

system include low cost and high methanol selectivity. Copper–zinc oxide interactions are considered crucial for the state of Cu phase and thus for the catalytic activity [8, 9, 10]. Methanol dehydration occurs on an acid catalyst. Zeolite based catalysts have several advantages for methanol dehydration to DME. For instance, zeolite-type catalysts exhibit better resistance to steam relevant to more conventional alumina. Thus, zeolites with controlled acidity, in particular ZSM-5, have been employed for direct dehydration of methanol to DME [11, 12].

Catalyst deactivation is currently the most important challenge of direct DME synthesis. It reduces the catalyst life-time, DME productivity and hinders implementation of this process on a larger industrial scale. Previous reports suggest that the deactivation of copper zeolite hybrid catalysts can be due to the following phenomena: copper sintering, copper oxidation and migration to the zeolite acid sites, coke deposition on both copper nanoparticles and zeolites or contamination by impurities in syngas [13, 14, 15, 16, 17, 18]. Because of the lack of direct characterization techniques working under harsh reaction conditions (high temperature and pressure), the information about deactivation mechanisms occurring in bifunctional Cu/ZSM-5 catalysts is rather contradictory. Catalyst removal and transfer from the catalytic reactor to the characterization equipment can significantly modify the copper oxidation state and whole catalyst structure.

Synchrotron-based techniques such as X-ray diffraction (XRD) and XANES/EXAFS provide important direct *in-situ* information about the structure of heterogeneous catalysts. High brilliance of synchrotron source allows acquiring time-resolved *in-situ* XRD patterns and X-ray absorption spectra even for diluted and dispersed systems exposed to high gas pressure. Previously, deactivation phenomena in cobalt Fischer-Tropsch catalysts were investigated with a greater precision using *in-situ* synchrotron-based techniques [19, 20, 21]

In the present work, the structure of copper-zeolite hybrid catalysts during activation and under realistic conditions of direct DME synthesis from syngas was investigated using a combination of

in-situ time-resolved XRD and XANES/EXAFS in the specifically designed experimental set up operating under high pressures and temperatures. The *in-situ* data are discussed together with the results of conventional *ex-situ* characterization and catalytic tests.

2. Experimental

2.1. Catalyst preparation

The hybrid catalyst for direct DME synthesis was prepared by physically mixing the powders (under 150 mesh) of the prepared Cu-Zn-Al methanol synthesis catalyst (CZA) and ZSM-5 zeolite (Si/Al=13, *Zeolyst*). The mechanical mixture of the CZA catalyst and zeolite (5:3 wt./wt.) was pressing into tablets, which were crushed into granules before the reaction. The ZSM-5 zeolite was characterized by low temperature nitrogen adsorption and NH_3-TPD. The zeolite textural characteristics are given in **Table 1**.

The CuO–ZnO–Al_2O_3 precursor (Cu:Zn:Al = 60:30:10 atomic ratio) was prepared by co-precipitation using a solution containing metal nitrates ($[Cu^{2+}]+[Zn^{2+}]+[Al^{3+}]$ =1.0 M) and a sodium carbonate solution at constant pH (ca. 7) and constant temperature (70 ˚C). The suspension was continuously stirred and kept at the desired pH by adjustment of the relative flow rates of the two solutions. The final suspension was aged under stirring at 70 ˚C for 1 h. The precipitate was filtered off, repeatedly washed with sufficient amounts of deionized water to remove residual sodium ions, dried at 110 ˚C overnight and then finally calcined at 350 ˚C in flowing air for 6 h yielding the oxide CuO–ZnO–Al_2O_3 (CZA) catalyst.

2.2. Ex-situ catalyst characterization

The zeolite and hybrid catalysts have been characterized at different preparation steps by a wide range of *ex-situ* techniques. The BET surface area, pore volume and average pore diameter were determined by low temperature N_2 adsorption using a Micromeritics ASAP 2000 automated system.

The NH_3-TPD curves were obtained in an Autochem 2910 equipment (Micromeritics) coupled with a quadrupole mass spectrometer (OmniStar from Balzers Instruments). Prior to ammonia adsorption, ca. 100 mg of the sample was pretreated at 500 °C for 60 min in He. The chemisorbed ammonia was then desorbed by heating from 50 °C to 1000 °C at a heating rate of 10 ˚C/min. The m/z = 16 signal in the coupled mass spectrometer was used to obtain the corresponding NH_3 desorption profiles.

The TEM analysis was carried out on a Jeol 2100F (field emission gun) microscope operating at 200 kV equipped with a probe corrector for the spherical aberrations.

The catalyst reducibility was examined by temperature-programmed reduction (TPR) performed in an AutoChem II 2920 apparatus (Micromeritics). The samples were reduced in a flow of 5 % H_2/Ar flow (60 ml/min) and heated up to 900 °C with the ramping rate of 10 °C /min.

2.3. In-situ catalyst characterization

The *in-situ* time-resolved XRD and XANES/EXAFS data in the transmission mode were simultaneously measured at the BM01B beamline (ESRF, France) using a high-resolution diffractometer, a gas manifold system and a capillary reactor. The experimental setup was described in detail in previous reports [19, 20, 21]. The copper-zeolite hybrid catalyst (3-5 mg) was loaded in the quartz capillary (OD=1 mm, wall thickness=0.02 mm) and pressed from both sides with quartz wool. The setup has zero dead volume and allows maintaining constant very low gas

velocities (~1-2 ncm^3/min) indispensable for conducting experiments in the capillary cell reactor at high pressure. Before the *in-situ* tests, the catalysts were reduced in hydrogen flow at 290 °C under atmospheric pressure. The *in-situ* time-resolved XANES/EXAFS XRD patterns were recorded under gas flows at desired temperatures and pressures. The experimental conditions were the same as in the reactor set up used for evaluation of the catalytic performance. The measuring times of an XRD pattern or an XAS spectrum were respectively 10 min and 5 min. In the co-feeding experiments, water purged from air was added to the reactor with the rate of 0.5 cm^3/h using a Harvard syringe pump. In this work, copper metal crystallite sizes were calculated from broadening *in-situ* XRD patterns. Note that for the metal particles larger than 1.5-2 nm, the EXAFS nearest neighbor metal coordination numbers are not sensitive to the sizes of metal clusters [22].

2.4 Catalytic tests

The conventional DME synthesis catalytic tests were carried out in a fixed-bed stainless-steel tubular reactor (d_{int} =8 mm). Before reaction, the sample was reduced in hydrogen flow at 290 °C. The catalytic tests were conducted at 260 °C, total pressure of 20 bar, H_2/CO ratio in syngas of 2 and different gas-space velocities.

3. Results and discussion

3.1. Structure of catalyst precursors

CuO and ZnO diffraction peaks were observed in the XRD patterns of the calcined CZA catalyst. No diffraction peaks of the Al_2O_3 phase were present even at the aluminum content of 10 %. This suggests that aluminum oxide is present in the amorphous form. The TPR profile measured for the CZA catalyst is shown in **Figure 1**. The hydrogen consumption area observed between 200 and 330 °C was attributed to the reduction of CuO into metallic copper. The characterization results for

the CZA methanol synthesis catalyst are consistent with previous reports [23, 24, 25]. The parent ZSM-5 zeolite showed the ammonia desorption at two temperatures: a low-temperature peak at 100-300 °C and a high-temperature peak at 400-600 °C corresponding respectively to the weaker and stronger acid sites. The total amount of acid sites was 993 μmol/g (**Table 1**).

The catalytic data in direct DME synthesis over the hybrid CZA/ZSM-5 catalysts measured in a conventional catalytic setup are presented in **Figure 2**. The reaction was conducted at 260 °C, total pressure of 20 bar. The DME selectivity was over 60%, while the selectivity to CO_2 was about 30 %. In direct DME synthesis, CO_2 is produced by the WGS reaction: $CO+H_2O=CO_2 + H_2$. The methanol and hydrocarbon selectivities (mostly methane) were about 4 %. Carbon monoxide conversion at different gas space velocities slowly decreased with time on stream. This suggests that Cu-zeolite hybrid catalyst exhibits noticeable deactivation. Note that the reaction selectivity is only slightly affected by the deactivation. The observed catalytic performance and catalyst deactivation are consistent with previous reports [17, 18]. In order to shed light on the evolution of the catalyst structure during the catalyst activation in hydrogen and exposure to syngas, we conducted *in-situ* synchrotron based X-ray absorption and diffraction experiments.

3.2. In-situ X-ray absorption and X-ray diffraction characterization

The XANES spectra and EXAFS Fourier transform moduli of the CZA/ZSM-5 hybrid catalyst during its reduction are presented in **Figure 3a and 3b**. The XANES spectrum of oxidized hybrid catalyst resembles the spectrum of bulk CuO. The XANES spectrum of CuO has two distinguishable features characteristic of Cu^{2+} ($3d^9$) complexes with a small pre-edge absorption at 8978 eV and a shoulder at 8986 eV, which is assigned to the 1s-4p "shake down" transition [23, 26]. The Fourier transform moduli of EXAFS for the calcined copper zeolite hybrid catalyst are also similar to the reference spectrum of crystalline CuO (**Figure 3b**). Broader and lower intense

radial distribution peaks for the second and third CuCu coordination shells in the calcined catalysts indicate smaller sizes of CuO particles compared to bulk copper oxide and a more significant Debye-Waller factor. Heating the CZA/ZSM-5 hybrid catalyst in hydrogen flow results in significant modifications of the XANES spectra and Fourier transform moduli. The XANES spectra show a major decrease in the intensity of white line, which corresponds to the formation of copper metallic phase (**Figure 3a**). Both XANES and Fourier transform modulus suggest that after treatment in hydrogen, the copper local environment in the catalyst reduced at 160 °C gets very similar to that in metallic copper.

The conclusion about the important concentration of copper metallic phase in the reduced sample is also consistent with the *in-situ* XRD data. The XRD patterns of the oxidized hybrid catalyst show the peaks attributed to CuO, ZnO and ZSM-5 zeolite. After heating in hydrogen at temperatures higher than 180 °C, new intense peaks attributed to Cu fcc (**Figure 4**) appear. The catalyst reduced at 290 °C, clearly shows characteristic peaks of Cu fcc metallic phase along with the peaks of the ZSM-5 zeolite. Cu fcc is the only copper phase detected by XRD in the reduced catalysts. The results are in agreement with the catalyst XANES/EXAFS (**Figure 3a and b**) and TPR for the CZA catalyst (**Figure 1**) showing copper reduction occurring during temperature ramping in diluted hydrogen (5%H_2/Ar) between 200 and 330 °C.

Figure 5 shows TEM images of the oxidized CZA/ZSM-5 catalysts. Copper oxide nanoparticles of a few nm were clearly observed. The copper oxide crystallite sizes in the calcined catalyst calculated from XRD peaks broadening were in the range of 5-7 nm, while in the freshly reduced counterparts, the copper metallic crystallites have diameters of 9-10 nm. The observed increase in copper particle sizes after reduction compared to the sizes of CuO crystallites in the calcined catalysts (5-7 nm) is consistent with previous studies [23]. This indicates copper sintering, which occurs already during copper reduction. Indeed, if no copper sintering happened during the catalyst

reduction, calculation using molar volume of CuO and Cu suggests that the copper particle size after the reduction should decrease by 60 % but not increase. Importantly, no further modifications of the *in-situ* XRD patterns were observed after extended heating of CZA/ZSM-5 in hydrogen at 290 °C.

After activation in hydrogen, the following experiments were conducted with the copper-zeolite hybrid catalyst under the conditions of direct DME synthesis in the conventional fixed bed reactor and under total pressure of 20 bar.

After the reduction, the catalyst in the capillary (4 mg) was exposed to the syngas (H_2/CO=2) at atmospheric pressure and 120 °C. Then the system was pressurized up to 20 bar and temperature of the catalyst was risen up from 120 °C to 260 °C. In the first set of experiments, the catalyst was exposed to syngas with high gas space velocities (GHSV=90 000 cm^3/g_{cat} h). Noteworthy, no modifications of the XANES spectra were observed during the exposure to H_2/CO (**Figure 6**). The *in-situ* XANES spectra measured are almost identical. The XANES shapes are similar to reference copper foil indicating the presence of mainly metallic Cu in the sample at the reaction conditions. This suggests that no copper oxidation occurs.

The *in-situ* XRD analysis (**Figure 7a**) provided important information about modification of copper dispersion under these reaction conditions. As expected, Cu (111) XRD peak slightly shifts to smaller 2 Theta angles as a function of temperature, which is attributed to the increase in unit cell parameter. Note that the Cu unit cell parameter changes with the temperature from 120 to 260 °C because of the thermal expansion [27] of copper nanoparticles. In addition, a progressive narrowing of XRD copper fcc (111) peaks was observed. Copper sintering could be the most probable reason of the narrowing of Cu (111) XRD peaks. The mean diameters of copper fcc crystallites calculated from XRD patterns using the Scherrer method are displayed in **Figure 7b**.

The copper crystallite size increases from 9 nm to 12 nm as the copper-zeolite hybrid catalyst was heated in the flow of syngas at 120-260 °C temperature range.

In the second set of experiments, the syngas before entering the quartz capillary containing the catalyst (3.5 mg) passed through a stainless steel pre-reactor filled with the same CZA-ZSM-5 catalyst (100 mg). The catalyst pre-bed allowed us obtaining much lower gas space velocity (GHSV) without reducing the total gas flow rate. This is achieved by setting an additional catalyst bed heated at the same temperature upstream of the quartz capillary. The gas space velocity calculated taking into account the total amount of the catalyst in the pre-reactor and quartz capillary was 3600 cm^3/g_{cat}·h, which is close to the conventional GHSV used in direct DME synthesis [17] No change was observed in XANES spectra (**Figure 6**). This result confirms that the copper still remains in metallic state. At the same time, XRD analysis shows narrowing of the patterns attributed to copper metallic phase (**Figure 8a**). XRD peaks broadening analysis suggests an increase in copper crystallite size to 16 nm during the first 4 h of the reaction (**Figure 8b**). The increase in copper particle size seems to be more significant in the experiments with lower than with higher gas space velocity (d_{Cu}=17 nm versus d_{Cu}=12 nm). One of the possible explanations of the larger copper nanoparticles in the experiments with lower gas space velocity could be due to the presence of water generated during the DME synthesis, which could accelerate copper sintering and lead to larger copper nanoparticles. Note however, that even at higher CO conversion the pressure of water in DME synthesis could be rather moderate, because of significant water gas–shift reaction.

In order to confirm further the effects of water on copper sintering, additional experiments were conducted at higher water pressure. In these experiments, water was intentionally added to the catalytic reactor. The setup contained a stainless steel pre-reactor heated at 260°C and filled with CZA-ZSM-5 (100 mg). After conducting the *in-situ* test with dry syngas, water with the rate of 0.5

cm^3/h was co-fed to the reactor. The water co-feeding corresponded to the following composition of the reactor feed gas ($H_2/CO/H_2O$=2/1/5). The pressure of the introduced water was 12 bar. Co-feeding with water leads to higher rate of water gas shift reaction and higher production of CO_2. The effect was studied in detail in our recent work [18]. Addition of water resulted in further noticeable narrowing of copper XRD patterns (**Figure 8a**). The calculated copper particles size in the presence of water increased to 20 nm (**Figure 8b**). Note that the copper crystallite sze was about 9 nm in the activated catalyst. Analysis of the *in-situ* XRD data obtained both at high and low gas space velocities and with water co-feeding points out that, the stability of copper nanoparticle could be strongly affected by water pressure. Higher water pressure results in more significant copper sintering. Surprisingly, the reacting atmosphere has almost immediate effect on the size of copper nanoparticles. This suggests that kinetics of coper sintering is very fast under the conditions of DME synthesis. Note that no copper sintering was observed in the DME synthesis experiments previously conducted under atmospheric pressure [28]. Indeed, conducting reaction at atmospheric pressure should significantly reduce the water pressure even at the same carbon monoxide conversion and thus the rate of copper sintering.

The *in-situ* results are also consistent with the *ex-situ* characterization of the spent catalyst conducted using high resolution TEM, which revealed significant copper sintering (**Figures 9** and **10**). In the catalyst freshly activated in hydrogen, Cu-based nanoparticles, which are homogenously distributed on the plate-like structures with sizes of about 10 nm or inferior, were observed. The small ZnO platelets are locally covered by very thin layers (1-2 nm) of Cu; these layers do not extend over the entire external surface of the support grain. The yellow arrows points to nanoparticles from the grains. In the catalyst exposed to the DME synthesis reaction (**Figure 10**), the copper nanoparticles are significantly larger (superior to 20 nm) than for the initial

specimen. No small nanoparticles or thin layers were identified on the supporting grains, most probably due to Cu migration under the reaction conditions.

Thus, copper sintering under the conditions of DME synthesis has been shown by both *in-situ* and *ex-situ* characterization. The most important finding obtained using the *in-situ* characterization is relevant to the kinetics of copper sintering. Our data indicate very fast kinetics of copper sintering. The final size of copper nanoparticles is strongly affected by the presence of water.

In addition to rapid deactivation, the copper zeolite hybrid catalyst also exhibits longer-term deactivation for dozen hours on stream (Figure 2). Note that the deactivation of copper zeolite catalysts in direct DME synthesis may involve several mechanisms. Though copper sintering obviously contributes to the overall catalyst deactivation, the longer-term deactivation after 100 h of reaction (Figure 2) is strongly influenced by other phenomena. As suggested in the previous reports [17], these deactivation mechanisms may involve copper migration inside the zeolite with ion exchange with the zeolite hydroxyl groups. Coke deposition in the zeolite pore and over copper metal species [29] leading to the catalyst deactivation cannot be also excluded in particular, at longer reaction time.

Conclusion

The *in-situ* synchrotron experiments performed during catalyst activation and under the realistic conditions of direct DME synthesis (high pressure, 260°C) in combination with the conventional *ex-situ* characterization unambiguously uncovered rapid copper sintering in the hybrid copper-zeolite catalysts, while no copper oxidation was detected. Copper is always present in the metallic state under a wide range of reaction conditions. Copper sintering, which proceeds with a very high rate, leads to larger particles in the presence of more significant amounts of water. The *in-situ* data are consistent with the results of *ex-situ* characterization of spent catalysts. Copper sintering could

be one of key factors responsible for the rapid short-term deactivation of copper zeolite hybrid catalysts during direct DME synthesis from syngas.

Acknowledgements

The authors are thankful to Dr. W. van Beek for the help with synchrotron experiments. The support of the French National Research (CATSYN-BIOFUELS project, ANR-12-BS07-0029) is gratefully acknowledged. M. C. thanks China Scholarship Council for the PhD stipend. The European Synchrotron Radiation Facility is acknowledged for providing synchrotron beam time.

Reference

1 G.A. Olah, Angew. Chem., Int. Ed. 52 (2013) 104-107.

2 J. Sun, G. Yang, Y. Yoneyama, N. Tsubaki, ACS Catal. 4 (2014) 3346-3356.

3 G. Yang, N. Tsubaki, J. Shamoto, Y. Yoneyama, Y. Zhang, J. Am. Chem. Soc. 132 (2010) 8129-8136.

4 A. Serov and C. Kwak, Appl. Catal. B 91 (2009) 1-10.

5 G. R. Moradi, J. Ahmadpour, F. Yaripour and J. Wang, Can. J. Chem. Eng. 89 (2011) 108-115.

6 J.C.J. Bart and R.P.A. Sneeden, Catal. Today 2 (1987) 1-124.

7 G.C. Chinchen, P.J. Denny, J.R. Jennings, M.S. Spencer and K.C. Waugh. Appl. Catal. 36 (1988) 1-65.

8 M. Günter, T. Ressler, B. Bems, C. Büscher, T. Genger, O. Hinrichsen, M. Muhler and R. Schlögl, Catal. Lett. 71 (2001) 37-44.

9 J. Wagner, P. Hansen, A. Molenbroek, H. Topsøe, B. Clausen and S. Helveg, J. Phys. Chem. B 107 (2013) 7753-7758.

10 P. Hansen, J. Wagner, S. Helveg, J. Rostrup-Nielsen, B. Clausen and H. Topsøe, Science 295 (2002) 2053-2055.

11 V. Vishwanathan, K.-W. Jun, J. W. Kim and H. S. Roh, Appl. Catal. A 276 (2004) 251-255.

12 J. Fei, Z. Hou, B. Zhu, H. Lou and X. Zheng, Appl. Catal. A 304 (2006) 49-54.

13 A. García-Trenco, A. Martínez, Appl. Catal. A 493 (2015) 40-49.

14 A. García-Trenco, A. Vidal-Moya, A. Martínez, Catal. Today 179 (2012) 43-51.

15 I. Sierra, J. Ereña, A.T. Aguayo, J.M. Arandes, M. Olazar and J. Bilbao, Appl. Catal. B 106 (2011) 167-173.

16 D.-S. Wang, Y.-S. Tan, Y.-Z. Han and N. Tsubaki, J. Fuel Chem. & Techn. 36 (2008) 171-175.

17 V.V. Ordomsky, M. Cai, V. Sushkevich, S. Moldovan, O. Ersen, C. Lancelot, V. Valtchev and A.Y. Khodakov, Appl. Catal. A 486 (2014) 266-275.

18 M. Cai, V. Subramanian, V. V. Sushkevich, V.V. Ordomsky and A.Y. Khodakov, Appl. Catal. A 502 (2015) 370-379.

19 H. Karaca, J. Hong, P. Fongarland, P. Roussel, A. Griboval-Constant, M. Lacroix, K. Hortmann, O.V. Safonova and A.Y. Khodakov, Chem. Commun. 46 (2010) 788-790.

20 M. Sadeqzadeh, H. Karaca, O.V. Safonova, P. Fongarland, S. Chambrey, P. Roussel, A. Griboval-Constant, M. Lacroix, D. Curulla-Ferré, F. Luck and A.Y. Khodakov, Catal. Today 164 (2011) 62-67.

21 N.E. Tsakoumis, A. Voronov, M. Ronning, W. V. Beek, O. Borg, E. Rytter and A. Holmen, J. Catal. 291 (2012) 138-148.

22 R. R. Benfield, J. Chem.Soc, Faraday Trans.88 (1992), 1107-1110.

23 J .M. Beiramar, A. Griboval-Constant and A. Y. Khodakov, ChemCatChem 6 (2014) 1788-1793.

24 C. Baltes, S Vukojevic and F. Schuth, J. Catal. 258 (2008) 334-344.

25 J. L. Li and T. Inui, Appl. Catal. A 137 (1996) 105-117

26 J. Wang, P.A. Chernavskii, A.Y. Khodakov, Y. Wang, J. Catal 286 (2012) 51-61.

27 Thermal Expansion: Metallic Elements and Alloys, Y. S. Touloukian, R. K. Kirby, R. E. Taylor, P. D. Desai in :Thermophysical Properties of Matter, Vol. 12, 1st Edition, IFI/Plenum; 1 edition (1975) p. 1440

28 K.B. Kabir, H.E. Maynard-Casely and S. Bhattacharya, Appl. Catal. A 486 (2014) 49.

29 H. Zhang, W. Li, W. Xiao, International Journal of Chemical Reactor Engineering 10(2012) A82.

Table 1. Physico-chemical characteristics of the parent ZSM-5 zeolite

Catalyst	Si/Al ratio	Al content (mmol/g)	S_{BET} (m^2/g)	V_{mic}, (cm^3/g)	$V_{tot\ (<350\ nm)}$ (cm^3/g)	TPD (NH_3) (μmol/g)
ZSM-5	13	1.28	432	0.17	0.23	993

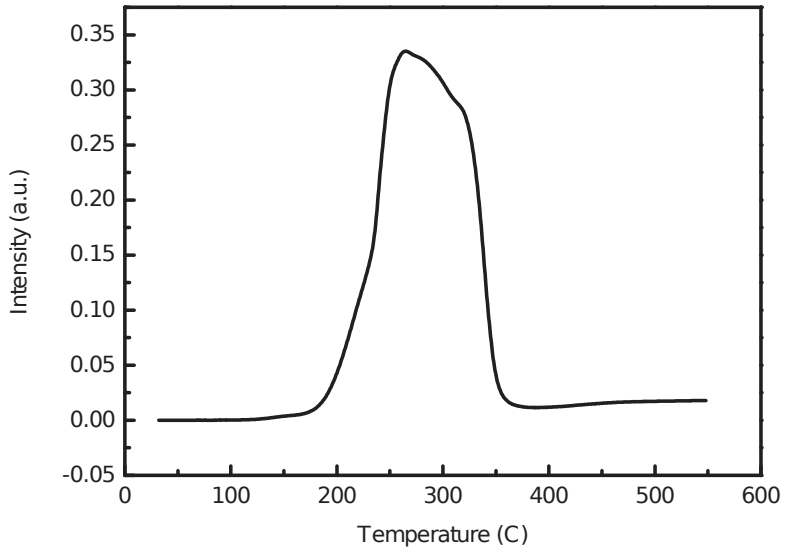

Figure 1. TPR profile of CZA catalyst

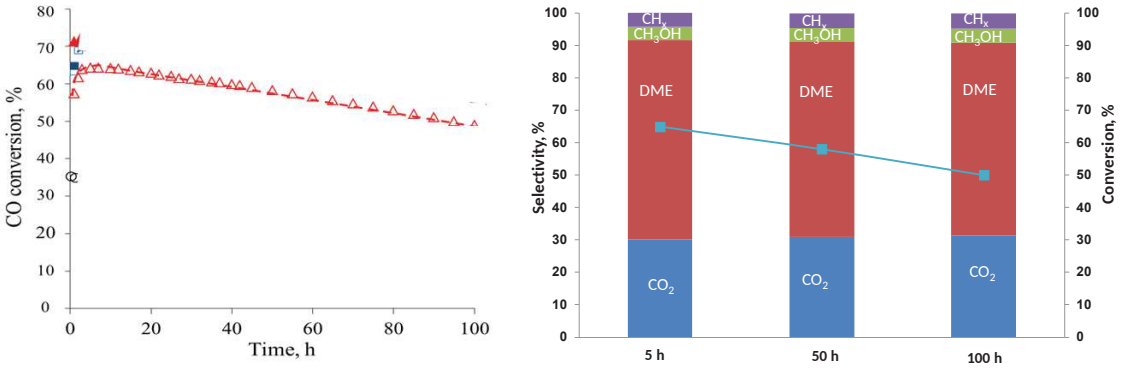

Figure 2. Variation of carbon monoxide conversion and selectivity during direct DME synthesis on CZA/ZSM-5 hybrid catalyst (T=260 ˚C, 3600 cm^3/g_{cat}^{-1} h^{-1}, $H_2/CO=2$, 20 bar)

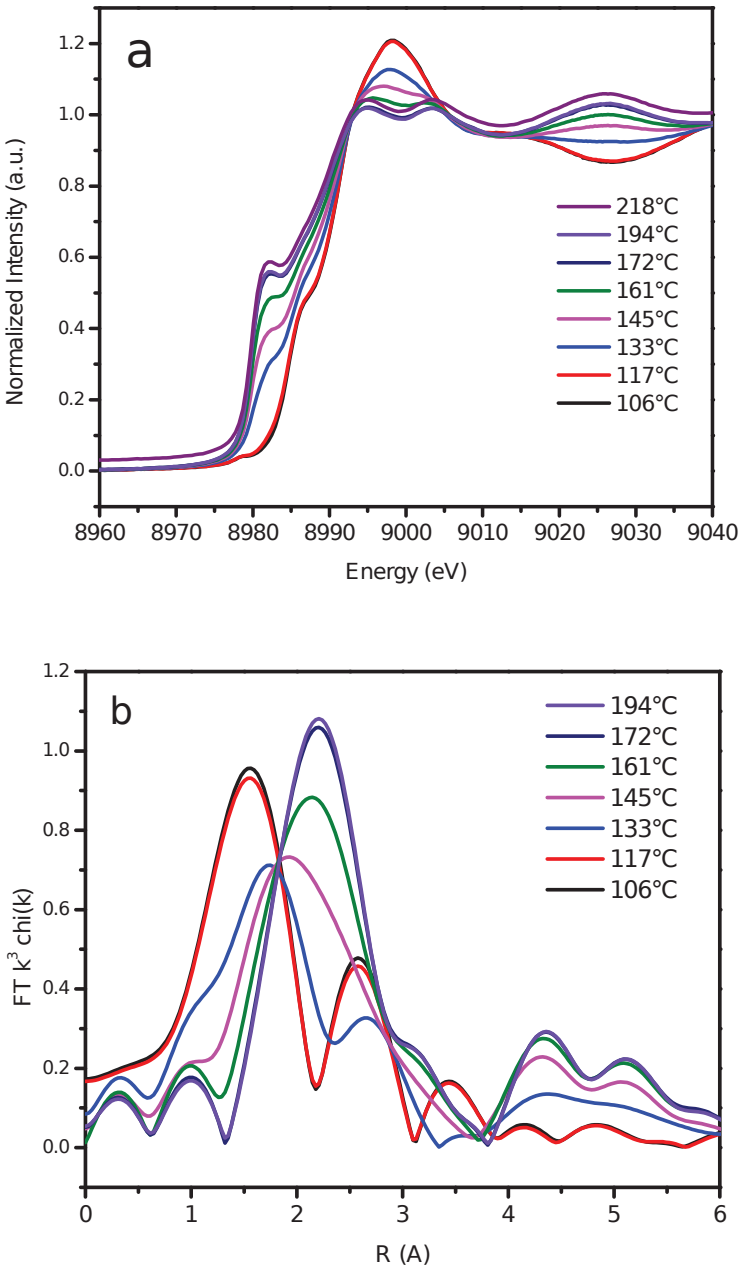

Figure 3. *In-situ* Cu K-edge XANES and Fourier transform EXAFS measured during reduction of the CZA/ZSM-5 hybrid catalyst

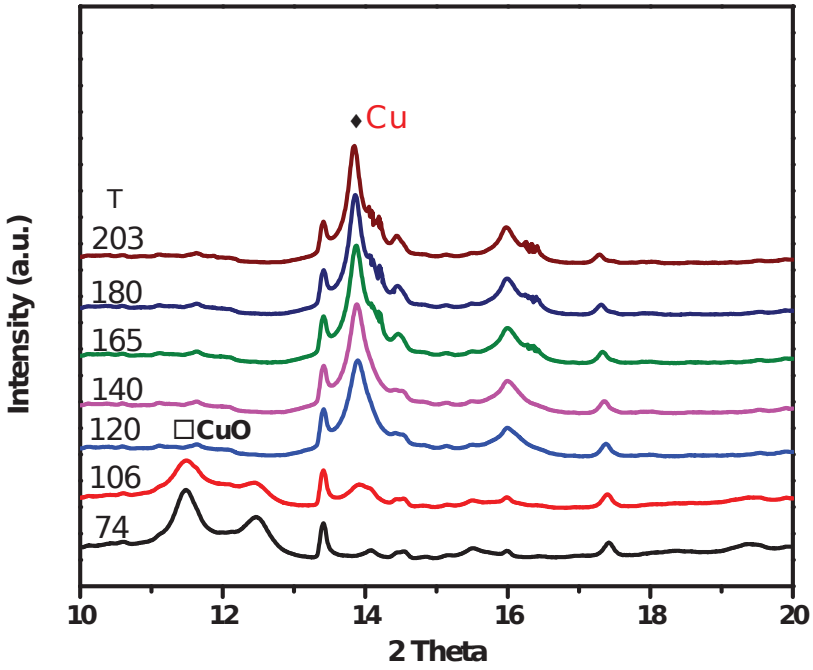

Figure 4. *In-situ* XRD patterns measured during reduction of the CZA/ZSM-5 catalyst (λ=0.05 nm)

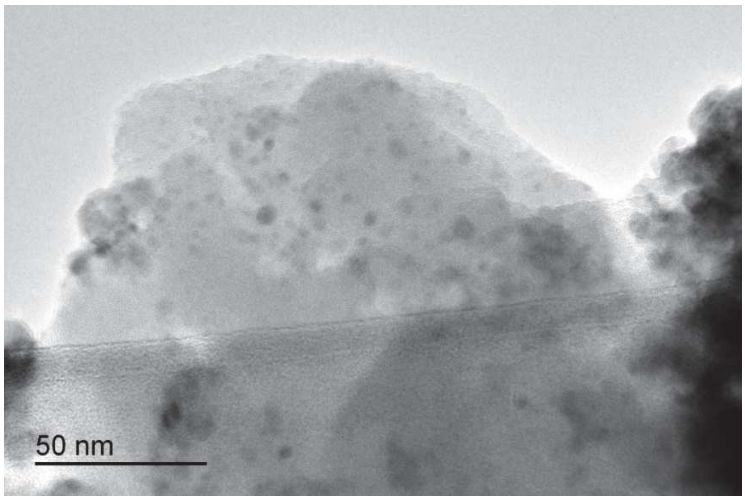

Figure 5. TEM images of the oxidized CZA/ZSM-5 catalyst showing the presence of copper nanoparticles.

Figure 6. Characteristic *in-situ* Cu K-edge XANES spectra of the CZA/ZSM-5 catalyst in syngas at P=20 bar and 260 °C measured in the in-situ DME synthesis experiments with low and high gas space velocities and with water co-feeding. All the spectra were identical.

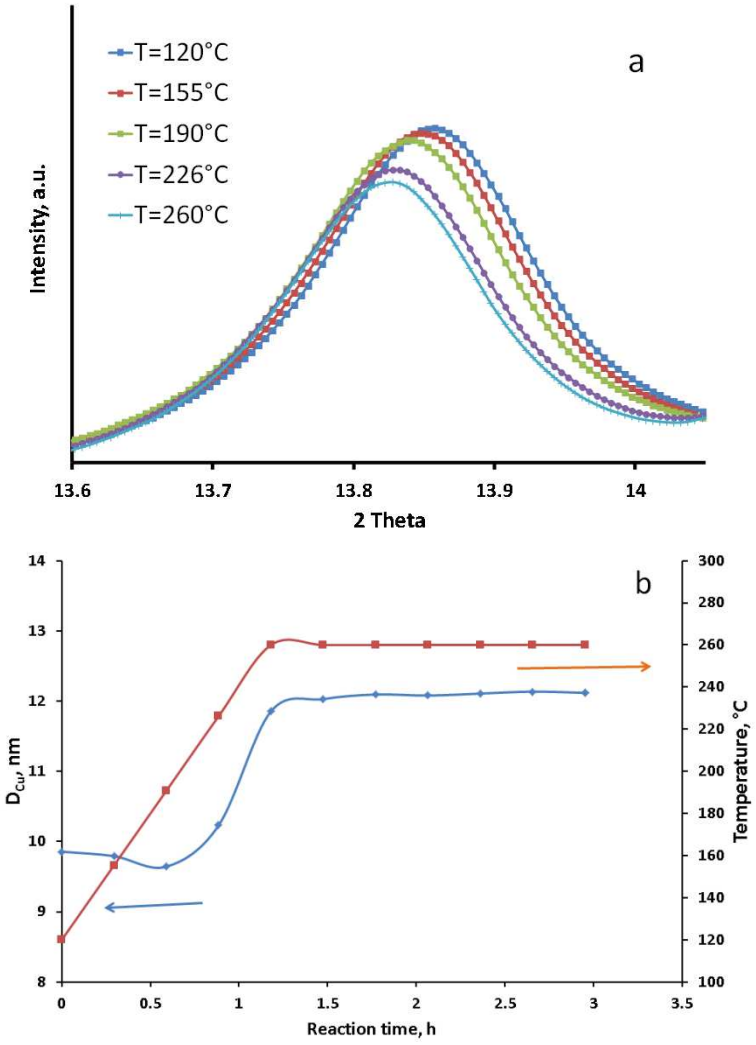

Figure 7. Evolution of the Cu (111) XRD peak (a) and copper metal nanoparticle size calculated using the Scherrer method (b) during direct DME synthesis at high gas space velocity (λ=0.05 nm, GHSV=90 000 cm^3/g_{cat} h, P=20 atm, T=260 °C, H_2/CO=2).

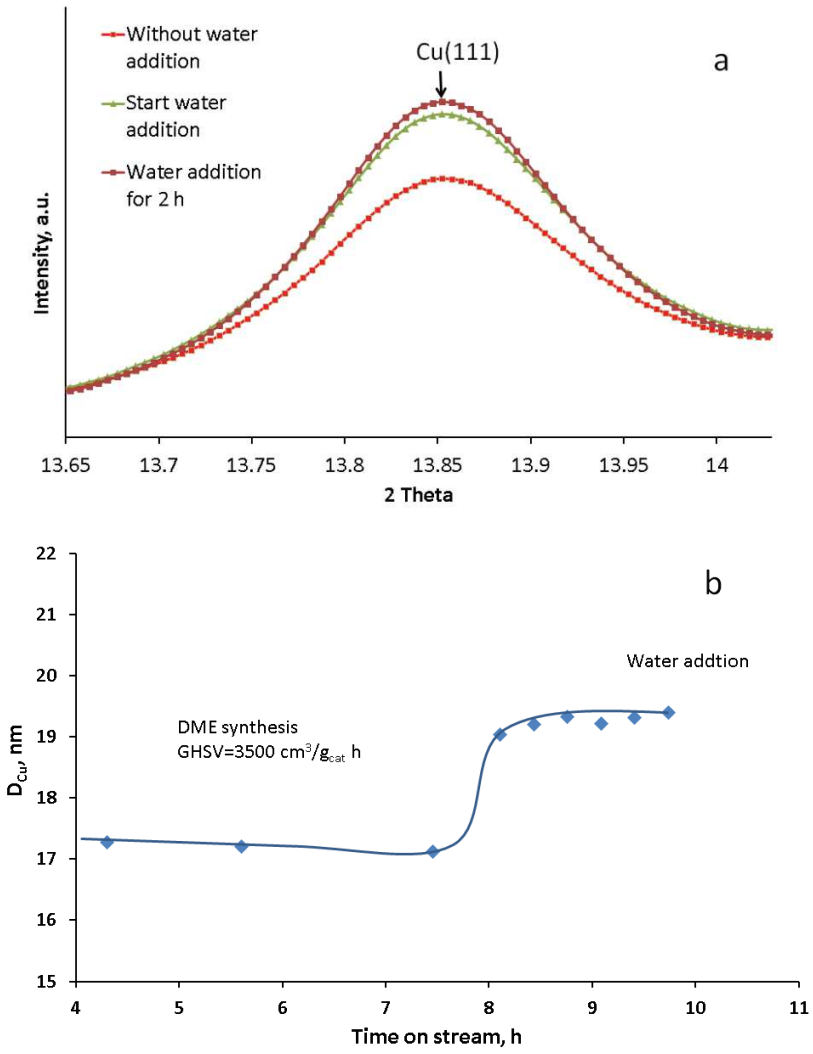

Figure 8. Evolution of the Cu (111) peak (a) and copper metal nanoparticle size calculated using the Scherrer method (b) during direct DME synthesis at low gas space velocity and with addition of water (λ=0.05 nm, GHSV=3 500 cm^3/g_{cat} h, P=20 atm, T=260 °C, $H_2/CO=2$ then water addition $H_2/CO/H_2O=2/1/5$, GHSV=9500 cm^3/g_{cat} h).

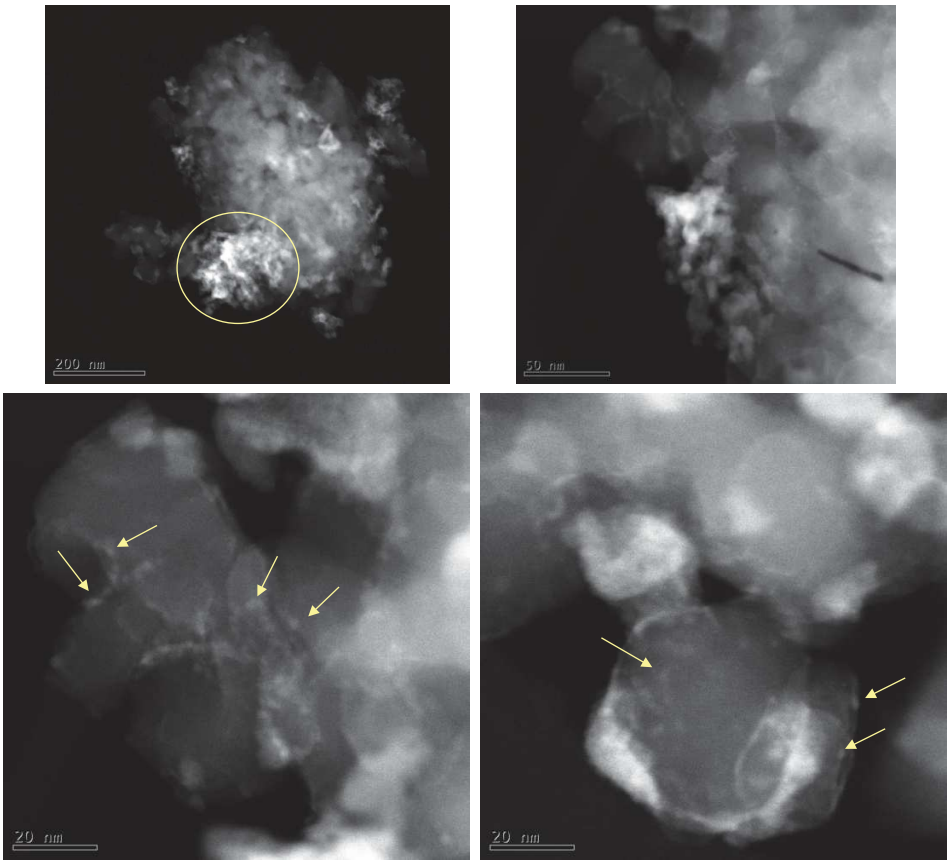

Figure 9. TEM images of CZA-ZSM5 after activation in hydrogen and before the catalytic reaction

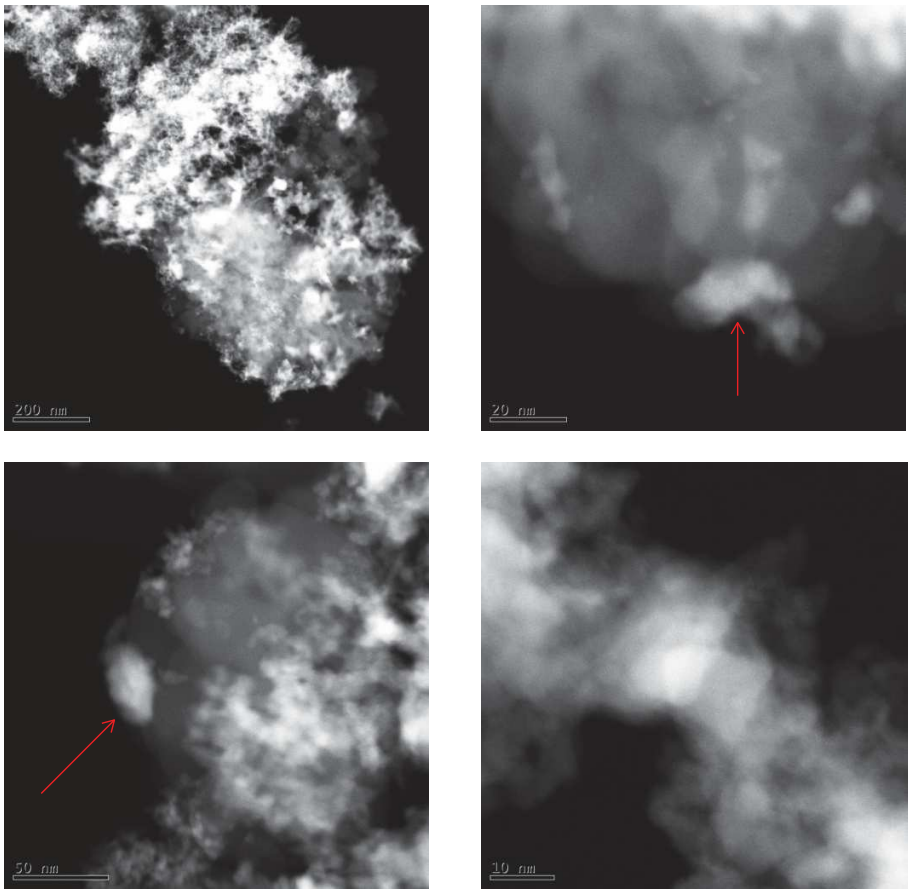

Figure 10. TEM images of CZA-ZSM5 after conducting direct DME synthesis (Conditions: T=260 ˚C, 3600 cm^3/g_{cat}^{-1} h^{-1}, $H_2/CO=2$, 20 bar)